DOR: 20.1001.1.25383620.2022.6.2.2.5

The Effect of Corrosion Intensity on Damage Metric in Impedance-Based Structural Health Monitoring of an Aluminum Cantilever Beam

A. Askari[1,] *, F. Hajami[2], V. Enjilela[3]

[1]Department of Mechanical Engineering, Nazarabad Center, Karaj Branch, Islamic Azad University, Karaj, Iran.
[2]Department of Industrial Engineering, Karaj Branch, Islamic Azad University, Karaj, Iran.
[3]Department of Mechanical Engineering, Karaj Branch, Islamic Azad University, Karaj, Iran.

Received: 21 August 2022 - Accepted: 11 November 2022

Abstract

Metal corrosion is the main phenomenon in different industries and destructive effects of this chemical phenomenon cause a lot of costs annually. While corrosion causes a little mass decrease in structure, brings about a dramatic reduction in mechanical strength and fatigue life of corroded materials. Hence, health monitoring of a structure can make aware of structure status at any time and prevents from harmful consequences. Structural Health Monitoring based on Electromechanical Impedance is one of the real-time monitoring techniques that could recognize damage on a structure by using an electromechanical coupling of piezoelectric materials, immediately. On the other hand, due to high frequency used in this method, small defects in the early stages will be detected. In this paper, Structural Health Monitoring based on Electromechanical Impedance was applied in an aluminum cantilever beam to recognize the corrosion and evaluate the capability of the Electromechanical Impedance method in detecting corrosion. Furthermore, the standard deviation of the mean square root has been chosen as the main metric, that it increases as the defect size increases. Afterwards, Experimental results were compared with health monitoring theory based on the Electromechanical Impedance and more energy method. Subsequently, the experimental results represent this method efficiency in the immediate monitoring of damage caused by corrosion in an aluminum cantilever beam. Besides, the possibility of pinpointing the defect by using this way has shown a good relationship between the place of damage and damage metric.

Keywords: Structural Health Monitoring, Cantilever Beam, Electromechanical Impedance, Damage Metric.

1. Introduction

Structural Health Monitoring is a research field with multiple applications that recently has attracted a numerous industrial and laboratory researches. Structural Health Monitoring evaluates the situation and health of the structure and manages to determine the recent situation of the structure and estimate its lifetime via interpreting the data. Structural Health Monitoring also measures and monitors the recent situation of the structure immediately [1]. Structural Health Monitoring is a powerful tool to save the costs of repair and maintenance that can reduce man-made errors. Structural Health Monitoring has got two ways: (1) Active Structural Health Monitoring (2) Passive Structural Health Monitoring. Passive Structural Health Monitoring measures diverse parameters of the structure and then by using these parameters determines the structural health. Active Monitoring is useful but cannot recognize the problem directly. For example, it cannot directly express if the structure has been damaged or not. On the contrary, Active Monitoring is in the relationship with structure Health's modes directly and this relation is for discovering the presence or developing of defect or damage.

**Corresponding author*
Email address: ali.askari@kiau.ac.ir

According to the description above, Structural Health Monitoring methods is similar to Non-Destructive Evaluating (NDE) methods, with this difference that Structural Health Monitoring method is a step ahead of NDE. In this step, Structural Health Monitoring tries to develop the sensors of finding damage in order to be installed on the structure and monitoring methods manage to monitor the receiving signals. The foremost part of Structural Health Monitoring system is related to the recall function of monitoring and a physical phenomenon contingent to the defect that is measured by sensor [1].

Structural Health Monitoring based on Electromechanical Impedance is a technique of recognizing the damage actively that uses intelligent substances material abilities in order to evaluate the structural health in a nondestructive way. The basic concept of this approach is monitoring the changes in mechanical impedance of the structure that is because of defect and damage such as corrosion or crack in the structure [2]. Since it is hard to measure the mechanical impedance of a structure, Structural Health Monitoring technique based on Electromechanical Impedance employs measuring the electrical impedance of the piezoelectric substances material. As is shown in Fig. (1). this electrical impedance is relevant to mechanical impedance the host

structure directly and is influenced by the presence of a defect in the structure.

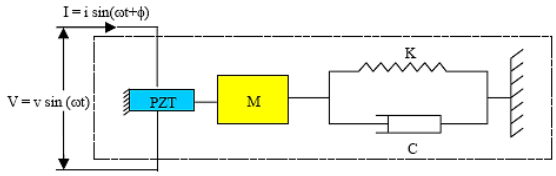

Fig.1. One degree of freedom to demonstrate structure dynamics by PZT.

Damage in a structure directly changes rigidity or dumping or both of the structure, and finally local dynamical properties will change, to wittiness: mechanical impedance changes with damage in structure. Because of the piezoelectric electrical impedance coupling with mechanical impedance, by measuring electrical impedance monitoring of piezoelectric and comparing it with the structure without defect, whether the structure has been damaged or is being damaged can be determined qualitatively. Up to now health monitoring technique based on electromechanical impedance has been conducted on several complicated structures and for diverse applications. Sun and his colleagues monitored the health of a Truss on 1995 [3], at the same time Chaudhry and et al. used this technique in order to monitor aviation structures [4]. Annamdas and Soh [5] reviewed some of the developments and applications of the EMI-based SHM (Structural health monitoring). The EMI technique provides several advantages over the traditional NDE approaches. First, because of the high-frequency range employed, the method is very sensitive to incipient damage in a structure and unaffected by changes in boundary conditions, loading, or operational vibrations. EMI technique can be used to quickly estimate the variations in the signatures. They predict that in the future, the EMI technique will also be better integrated with other techniques, especially wireless technology for more effective SHM. In 1996, Lalande and his colleagues applied this method to evaluate nondestructively exact and complicated structures with closed tolerance [6]. In this experiment, they evaluated the corrosion of gear wheel teeth. In 1999 Park and his coworkers evaluated the effect of temperature on the impedance and by introducing a damage metric they adjusted the temperature changes in the impedance [7] and at the same time Giurgiutiu and et al. [8] evaluated health on the spot welded joints of a structure. Park and et al. [9] evaluated the health of constructional structure components on 2000 [9] and at the same time Soh and et al. [10] evaluated the health of a reinforced concrete bridge. Park and et al. at 2001, [11] discovered the defect in pipelines using the Structural Health Monitoring technique based on electromechanical impedance. Corey Wilson [12] monitored the health of wind turbine blade successfully. At the same time Xing and his colleagues exerted this method in order to evaluate the impedance changes with damage growth and Fatigue crack [13]. Yang and et al. [14] employed this technique to monitor the health of cylindrical shells. An experimental study for wireless monitoring of corrosion damage that might frequently occur in metallic structures has been contrived by Park et al. [15] in 2010. A simple beam structure made from an aluminum alloy was selected for corrosion-monitoring testing, and a small PZT patch-type sensor was surface-mounted to the structure. To obtain an EMI data at the PZT sensor, a wireless impedance sensor node that consists of a miniaturized impedance-measuring chip, a microprocessor, and an RF telemetry was employed. Three different corrosion cases with a different corroded area were artificially inflicted on the beam structure using hydrochloric (HCI) acid, and the EMI data were collected in sequence from the wireless impedance sensor node. To quantify the corroded area, the variations of the resonant frequency that represents structural dynamic information were continuously tracked during all the damage cases. Conclusively, it has been found that the amount of the resonant frequency shift got increased when the corroded area got increased. The above experimental results verified that the proposed approach using the amount of resonant frequency shift at the measured EMI can be effectively utilized for quantitative analysis of the corroded area in metallic structures. The main purpose of Sepehry et al. [16] study in 2011 was to investigate the influence of variation of Piezoelectric wafer active sensors (PWAS) and structure constants with temperature on structural response in ISHM (impedance –based structural health monitoring). The theoretical model, based on the coupling of PWAS and structure for in situ structural health monitoring using energy methods has been proposed and applied to a beam. The temperature effect in this model is introduced by considering the material property temperature dependency of both aluminum beam and PWAS. In support of this model, experiments were conducted on an aluminum beam (alloy 2024) with integrated PWAS. It was shown that the measured electrical impedance of PWAS as a sensor around the structural natural frequencies was almost in agreement with those calculated by the proposed model. The experiments depict that the proposed model could correctly identify structural natural frequencies in the 16.5–33 kHz range. Theoretical and experimental results considering temperature variation are in agreement with each other. Increasing temperature, a left horizontal shift, and a decrease in amplitude of real of impedance in any natural frequencies have been observed in experimental results. The decrease in impedance amplitude is principally due to the PWAS constant

changes during temperature increase, while the horizontal shift of frequency to the left is because of aluminum constant changes with temperature increase. This validated model could be served further to predict the ISHM system response with different structural shapes and environmental conditions. Aluminum is a unique metal: strong, durable, flexible, impermeable, lightweight, corrosion-resistant and 100% recyclable. After steel, Aluminum is the most frequently used metal in the world and its uses continue to expand. Aluminum is amongst the most environmentally friendly metals on the planet. On a percentage basis, it is the most recycled of any industrial metal. Of the more than 1 billion tons of aluminum ever produced, roughly 75% of the most versatile and lightweight metal is still in use today thanks to recycling. Aluminum is an extraordinarily versatile material - it is easily machined, cast, drawn and extruded [17]. The electromechanical impedance method for health monitoring and the real-time diagnosis of corrosion defect in an aluminum tube was used by Akhoundi et al. [18] study. The results of this method in the real-time of corrosion defect indicate that by adding any defect to the aluminum tube, the change in impedance shape Electricity from piezoelectric has been clearly seen and the magnitude of damage is increased. Meanwhile, by increasing the defect, the magnitude of the damage is also increased, which indicates that there is a relationship between the amount of damage and the degree of defect, which is the depth of defect here. Fabricio et al. [19] investigated the effect of temperature on the electrical impedance signatures of a conventional 5H PZT sensor used in structural health monitoring in their study. The variations in both the amplitude and the frequency were analyzed experimentally by using an aluminum specimen and obtaining impedance signatures at temperatures ranging from 25 °C to 102 °C. The experimental results showed that the variations in the amplitude of the impedance signatures were related to the temperature-dependence of the capacitance of the piezoelectric sensor. In addition, the frequency shifts of the resonance peaks that resulted from temperature variations were not constant over the entire frequency range but increased with the frequency. Thus, the frequency band used to calculate the damage indices played an important role in compensating for temperature effects by maximizing the correlation coefficient. The results showed that a sufficiently narrow frequency band must be used to avoid a false positive diagnosis of the monitored structure. Therefore, temperature effects are a critical problem for structural health monitoring based on electromechanical impedance, especially in detecting low damage levels, and efficient compensatory methods for temperature effects remain to be developed. Rugina et al. [20], presented a self-contained study about E/M impedance methods for SHM thin circular plates. Comparisons between the analytical method, the finite element method, and experiments were performed, with fabricated structural arc-shape defects. Changes in the E/M impedance spectrum due to the presence of a crack were investigated. It is certified that the E/M impedance method presents the following advantages: small size of the permanently attached or embedded piezoelectric sensors, ultrasonic frequency range application, and ability to be used for online and in service SHM.

In this article, the health monitoring of a cantilever beam made of aluminum (1050 alloy) that is prone to corrosion has been evaluated and will be discussed over the possibility of pinpointing of the defect.

2. Materials and Methods

A cantilever beam made of aluminium (1050 alloy) was used to investigating the effect of Corrosion Intensity on Damage Metric in Impedance-Based Structural Health Monitoring. Once the impedance response is being planned, a qualitative approach to determining the defect is provided. Determining the quantitative defect is provided by a numerical damage metric. In this research, we use a statistical algorithm called Root Mean Square Deviation (RMSD). This algorithm mentioned in the Eq. (1)., is based on comparing frequencies [21].

$$M = \sum_{i=1}^{n} \left[\frac{\left(\mathrm{Re}\left(Z_{i,1}\right) - \mathrm{Re}\left(Z_{i,2}\right) \right)^2}{\mathrm{Re}\left(Z_{i,1}\right)^2} \right]^{\frac{1}{2}} \quad \text{(Eq. 1.)}$$

In which M represents damage metric, $Zi,_1$ is piezoelectric electrical impedance in the healthy mode in its frequency, $Zi,_1$ is piezoelectric electrical impedance in the recent mode in its frequency.

3. Detection of Corrosion in Cantilever Beam

In this section, Structural Health Monitoring experiment based on Electromechanical Impedance on an alloy aluminum 1050 beam and on the boundary conditions of the cantilever will be implemented. The dimension of the beam is $2 \times 25 \times 340$ millimeters. The properties of the beam have been brought to the Table. (1). below. The symbols used in this table have been shown in the Fig. (2). The frequency interval which involves so many peaks is between 12 to 22 kilohertz. In the cantilever beam condition, the clamp is applied first from one side of PZT and then from another side. The corrosive acid solution is a mixture of hydrochloric acid, nitric acid and sulfuric acid that

the amount of each has been shown in the Table. (4). in terms of volume percent.

Table. 1. Dimension and specification of cantilever beam in first test.

Parameter	Unit	Symbol	Quantity
Beam's effective length	Cm	L	33
Width	Cm	B	2.5
Thickness	Mm	H	2
Density	Kg/m^3	P	2700
Elasticity module	GPa	E	70

For better evaluation of distance effect and approximating the conditions, two experiments are done on a beam by using two PZT. Applied piezoelectric is made of PSI-5H4E and its sensor's dimensions are 0.267×20×20 millimeters.
The properties of piezoelectric have been brought in the following Table. (2). [22]. Meanwhile used symbols in this table have been shown in the Fig. (2).

Table. 2. PZT properties and parameters used in the first test.

Parameter	Unit	Symbol	Quantity
Length	Cm	L_p	2
Width	Cm	b_p	2
Thickness	Mm	h_p	0.267
Distance between the beginning of PZT and beam	Cm	X_1	1.5
Distance between the end of PZT and beam	Cm	X_2	$X_2 - X_1 = L_p$
Density	Kg/m^3	$_p\rho$	7749.985
Yield module	Pa^{-1}	S_{11}^E	1.64×10^{-11}
Strain coefficient	m/V	d_{31}	-320.026×10^{-12}
Dielectric constant	F/m	ε_{33}	$3800\varepsilon_0$
Dielectric constant in atmosphere	F/m	ε_0	8.85×10^{-12}

The frequency interval which involves so many peaks is between 12 to 22 kilohertz. In the cantilever beam condition, the clamp is applied first from one side of PZT and then from another side. The corrosive acid solution is a mixture of hydrochloric acid, nitric acid and sulfuric acid that the amount of each has been shown in the Table. (4). in terms of volume percent.

Table 4. Specification of solution used to impose corrosion.

Type	Acid H2SO4	Acid HCL	Acid HNO3
Percentage	10%	%40	%50

The shape of corrosion will be imposed as a rectangle with dimensions of 20×25 millimeters and behind the beam and in two different places with two different depths. In Fig. (2). the schematic and real picture of test beam with bound piezoelectric has been shown.

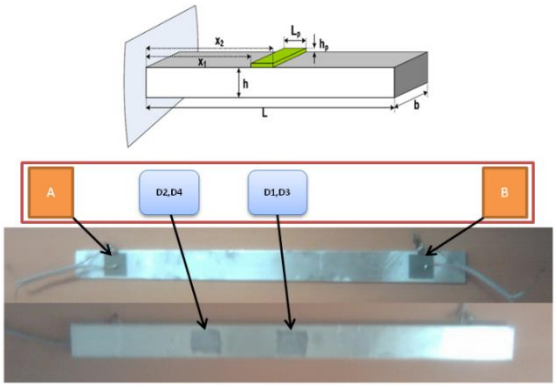

Fig. 2. Beam figures along with locality of developed defects.

Depths of corrosion respectively proportion to 10 and 20 percent of beam thickness in each place. The impedance measurement does occur first in the healthy mode and then after imposing each of the corrosions.

4. Results and Discussion

As is shown in the Fig. (3)., the cantilever beam is clamped from next to the PZT A and the data of Impedance obtained from PZT A, in the first boundary condition.

Fig. 3. Schematic layout of beam with piezoelectric and clamp.

The impedance diagram in the healthy mode in the Fig. (4). and impedance diagrams after adding different defects has been shown in the Fig. (5). To Fig. (8).
Fig. (4). shows the variation of real part impedance of the structure in the healthy condition in the frequency range 12 to 22 kHz. The peaks indicated

in the figure are the resonant frequencies of the structure.

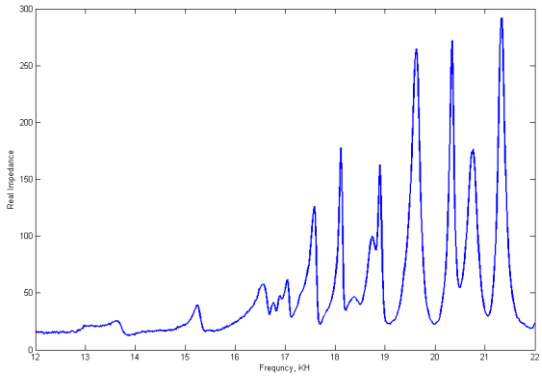

Fig. 4. The impedance of cantilever beam in healthy condition detected by PZT A.

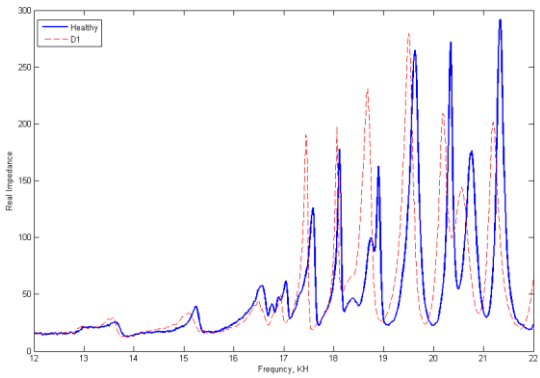

Fig. 5. The impedance of cantilever beam in a healthy condition and emergence of the first defect both detected by PZT A.

Figure 5 shows the changes in the real part of structure impedance in the flawless mode and after adding the first defect in terms of ohm and in the frequency range of 12 to 22 kHz. Changes in amplitude and frequency shift represent the defect existence or change in mechanical impedance of the structure.

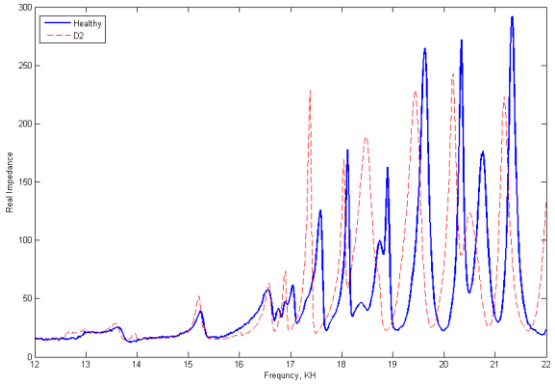

Fig. 6. Impedance of cantilever beam in healthy condition and emergence of second defect both detected by PZT A.

Figure 6 shows the changes in the real part of structure impedance in the flawless mode and after adding the second defect in terms of ohm and in the frequency range of 12 to 22 kHz. It is obvious that changes in amplitude and frequency shift in this mode are more than the previous mode. This means more changes in the created defect or more changes in mechanical impedance of the structure.

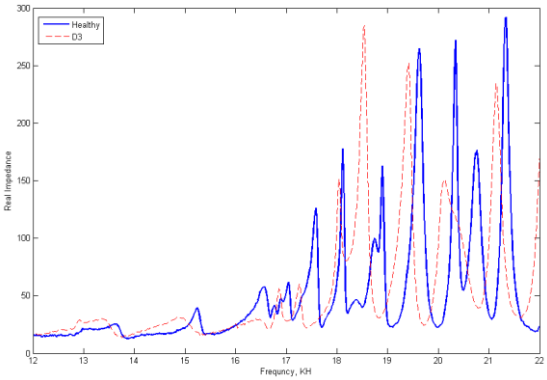

Fig. 7. The impedance of cantilever beam in a healthy condition and the emergence of third defect both detected by PZT A.

Figure 7 shows the changes in the real part of structure impedance in the flawless mode and after adding the third defect in terms of ohm and in the frequency range of 12 to 22 kHz. It is clear that changes in amplitude and frequency shift in this mode are more than the previous modes. This is because of adding the created defect in the structure or more changes in mechanical impedance of the structure.

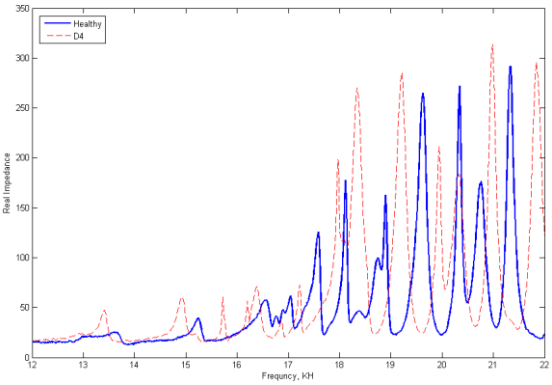

Fig. 8. The impedance of cantilever beam in a healthy condition and the emergence of forth defect both detected by PZT A.

Figure 8 shows the changes in the real part of structure impedance in the flawless mode and after adding the fourth defect in terms of ohm and in the frequency range of 12 to 22 kHz. It is clear that changes in amplitude and frequency shift in this mode are more than the previous modes. This is because of adding the created defect in the

structure or more changes in mechanical impedance of the structure. For more understanding, we have sketched all the impedance diagrams for the healthy and defective modes altogether in a small frequency range in the Fig. (9). As is obvious in the Fig. (9). the impedance diagram changes when adding each defect which is observed as frequency shift and change in amplitude. This change in the impedance diagram represents a change in mass, rigidity or structural damping and this means the structure has been changed or to wit, has been damaged. In the diagram of damage metric shown in Fig. (10). is observed that the damage metric rises after adding each defect.

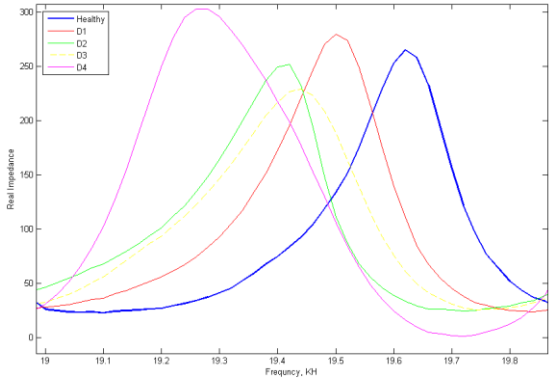

Fig. 9. The impedance of cantilever beam in healthy and defective condition in the frequency range between 19 and 20 kHz detected by PZT A.

Figure 10 shows the changes in the real part of structure impedance in the flawless mode and after adding the first, second, third and fourth defect in terms of ohm and in the frequency range of 19 to 20 kHz. It is obvious that adding each defect causes a change in amplitude and frequency shift.

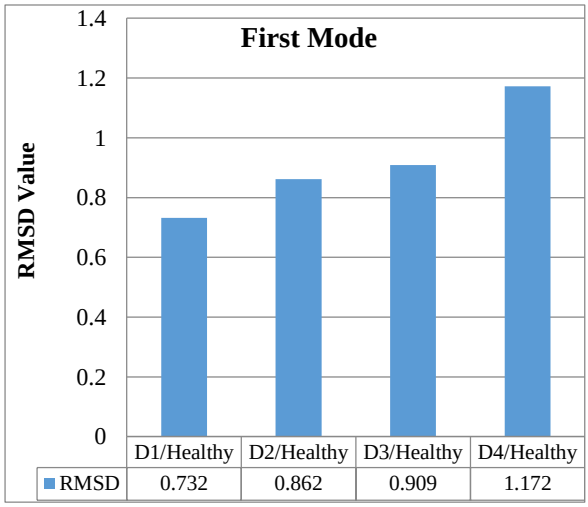

Fig. 10. Damage metric in cantilever beam detected by PZT.

In the next step as is shown in the Fig. (11)., the cantilever beam is clamped from next to the PZT B and the data of Impedance obtained from PZT B, in the second boundary condition.

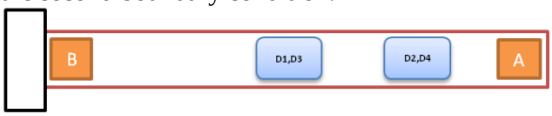

Fig. 11. Schematic layout of beam with piezoelectric and clamp.

The impedance diagram produced by piezoelectric B in the healthy mode in the Fig. (12). and the impedance diagrams for each defect have been sketched in the Fig. (13). to Fig. (16).

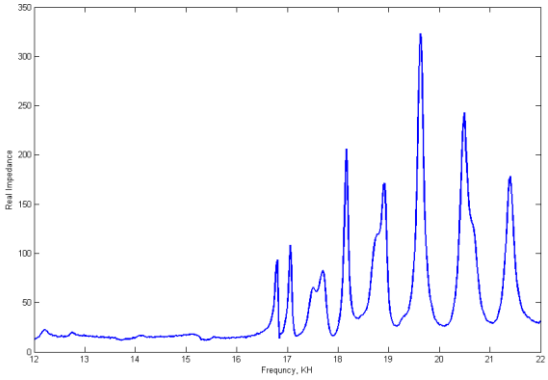

Fig. 12. The impedance of cantilever beam in healthy condition detected by PZT B.

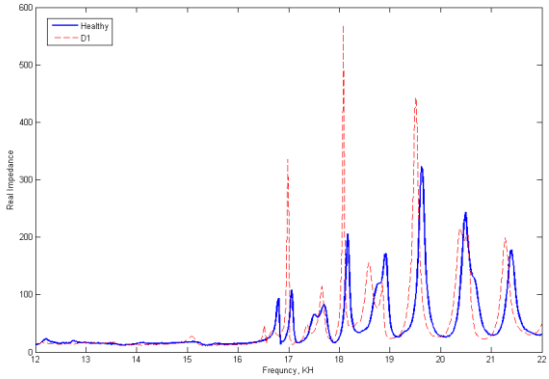

Fig. 13. The impedance of cantilever beam in a healthy condition and emergence of the first defect both detected by PZT B.

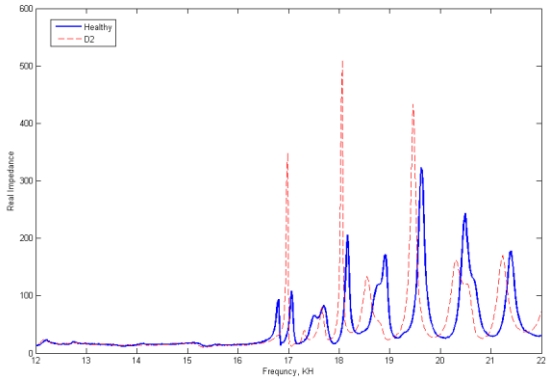

Fig. 14. The impedance of cantilever beam in a healthy condition and emergence of second defect both detected by PZT B.

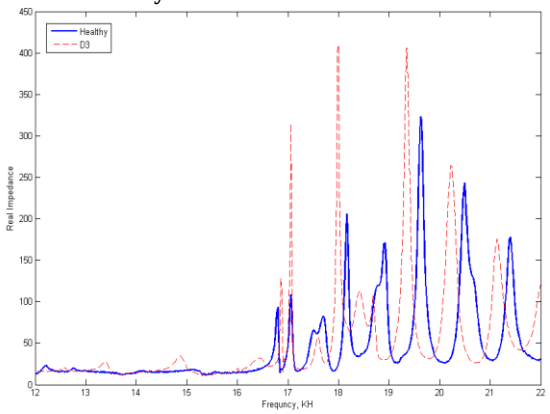

Fig. 15. The impedance of cantilever beam in a healthy condition and the emergence of third defect both detected by PZT B.

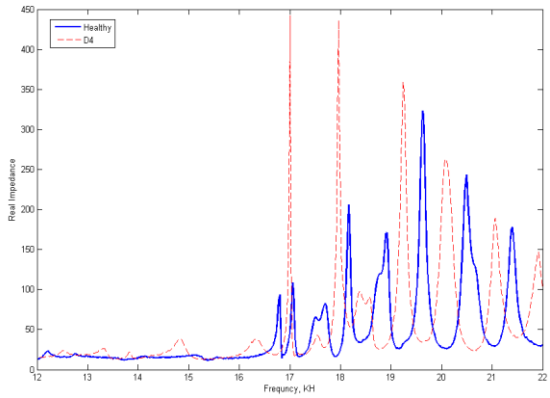

Fig. 16. The impedance of cantilever beam in a healthy condition and the emergence of forth defect both detected by PZT B.

As a further description, we have sketched all the impedance diagrams produced by piezoelectric B for the healthy and defective modes altogether in a small frequency range in the Fig. (17). In the diagram of damage metric shown in Fig. (18). is observed that the damage metric rises after adding each defect.

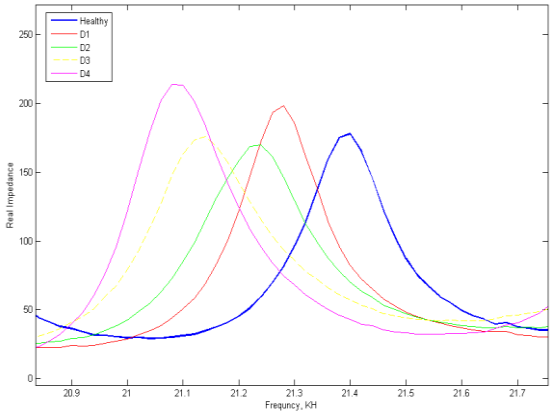

Fig. 17. The impedance of cantilever beam in healthy and defective condition in the frequency range between 20.8 and 21.8 kHz detected by PZT B.

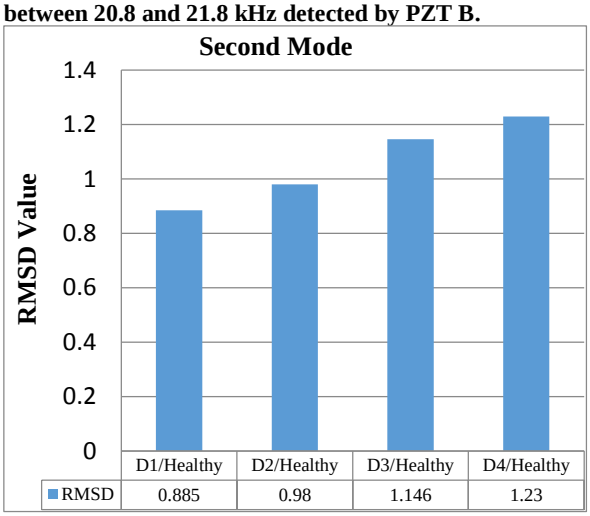

Fig. 18. Damage metric in cantilever beam detected by PZT B.

The damage metric represents the difference between two impedance diagrams. The more the damage metric is, the more the impedance diagram in the current status will change in comparison to the healthy mode and that will be observed as frequency shift or change in amplitude in the impedance diagram. In this experiment to evaluate the defect distance effect on the impedance diagram and the amount of damage metric, suffice to compare all the modes together mentioned in the previous section. Because in this case the clamping conditions are same and we can only maneuver on the effect of defect distance from piezoelectric. In the first mode of clamping is from the side of piezoelectric A and measuring impedance is done from this piezoelectric and in the next mode of clamping is from the side of piezoelectric B and measuring impedance is done from this piezoelectric. Fig. (19). shows a schematic view of the cantilever beam in the first and second modes.

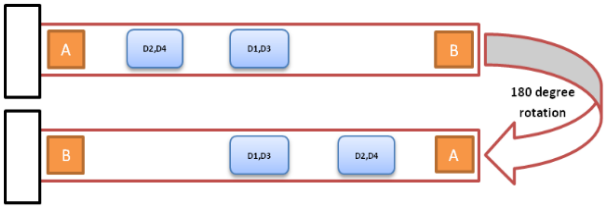

Fig.19. Schematic layout of beam with piezoelectric and clamp in first and second condition.

It is expected that the more the defect is close to piezoelectric, the more the changes in the impedance diagram are intense and consequently, the damage metric has a greater amount. Thus, in the first mode, the amount of damage metric must be more remarkable for defects D2 and D4 and this amount is greater for the defects D1 and D3 in the second mode. The amounts of damage metric have been shown in the Fig. (20).

Table. 5. Difference between damage metric for first mode in relative and absolute situation.

Factor	Difference btw. D1 & D2	Difference btw. D2 & D3	Difference btw. D3 & D4	Difference btw. D2 & D1	Difference btw. D1 & D3	Difference btw. D1 & D4
Quantity	17.73%	5.51%	28.19%	17.73%	24.22%	60.01%

Table. 6. Difference between damage metric for second mode in relative and absolute situation.

Factor	Difference btw. D1 & D2	Difference btw. D2 & D3	Difference btw. D3 & D4	Difference btw. D2 & D1	Difference btw. D1 & D3	Difference btw. D1 & D4
Quantity	10.68%	17%	7.24%	10.68%	29.5%	38%

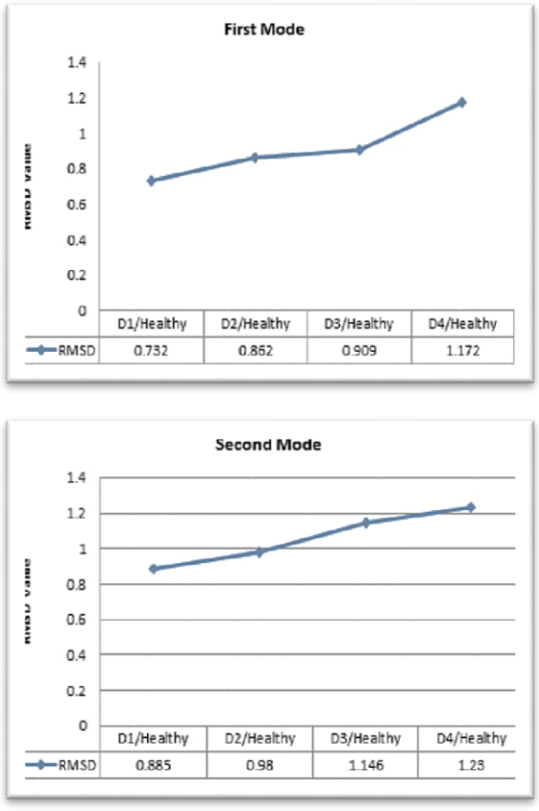

Fig. 20. Damage metric in first and second mode.

In the diagram relating to the first mode, it is observed that the diagram slope between mode D1 and D2 and mode D3 and D4 is more than diagram slope in the mode D2 and D3 and it means that the difference between impedance diagram has been more for second and forth defects.
To a better clarification, the inconsistency between the amounts of damage metric and the amount of the increase percent in the relative mode and absolute mode has been presented in the Table. (5). As is clear how much the defect is closer to the piezoelectric then the changes in the impedance diagram become greater. Consequently, it will result in a greater amount of damage metric and also cause more differences between each of the damages. In the diagram relating to the second mode (Fig. 20) which the quantities are described in Table. (6), also is observed that the slope amount between mode D2 and D3 is more than slope amount between mode D3 and D4 and this means the difference between the impedance diagram for the third defect is more than the others.
Besides, in this mode, it is obvious that more changes are produced in the impedance diagram because of the closeness of the defect D3 to the piezoelectric B that results in a greater amount of damage metric and consequently causes more difference between damages.

5. Conclusion

In this study, an electromechanical impedance method for monitoring health and the real-time diagnosis of corrosion defects in an aluminum alloy beam has been implemented. The experimental results obtained from the efficiency of this method in the real-time detection of flaws due to corrosion show that:
1- By adding any defect to the aluminum beam, the change in the shape of the impedance of the output of the piezoelectric circuit is clearly seen in the range of amplitude and frequency shift. This implementation is also to quantify the results of a damage criterion based on the frequency-to-frequency comparison.
2- The magnitude of this damage criterion is high by adding each defect to the pinch.
3- In the next study, the correlation between piezoelectric defect distance and damage criterion

is investigated. According to the empirical data obtained, it is concluded that the created defects are closer to the piezoelectric.
4- The damage criterion for these defects is much higher when compared with healthy beams.
5- Because of these defects are closer to the piezoelectric, it causes more changes in the impedance shape.
6- A further change in the shape of the piezoelectric output impedance means an increase in the value of the injury criterion.

References

[1] V. Giurgiutiu, "Structural Health Monitoring with Piezoelectric Wafer Active Sensors", Academic Press, Burlington, MA, (2008).
[2] C. Liang, F. P. Sun and C. A. Rogers, J. Intell. Mater. Syst. Struct., Vol. 5, 1994, 21.
[3] F. Sun, Z. Chaudhry, C. Liang, and C. A. Rogers, J. Intell. Mater. Syst. Struct., V.6, 1995, 134.
[4] Z. Chaudhry, F. Lalande, F. Ganino, C. A. Rogers and J. Chung, Proc. AIAA/ASME/ASCE/AHS/ASC 36th Struct., Struct. Dyn. Mater. Conf., Adaptive Structures Forum, AIAA Publish., (1995), 2243.
[5] Annamdas, Venu Gopal Madhav and Chee Kiong Soh., J. Intell. Mater. Syst. Struct., 21.1 (2010), 41.
[6] F. Lalande, B. Childs, Z. Chaudhry and C. A. Rogers, Proc. SPIE Conf. Smart Struct. Mater., SPIE Publish., V. 2717,(1996), 237.
[7] G. Park, K. Kabeya, H. Cudney, D. J. Inman, JSME Int. J., Vol.42, No.2, (1999), 249.
[8] V. Giurgiutiu, A. Reynolds and C. A. Rogers, J. Intell. Mater. Syst. Struct., Vol 10, (1999), 802.
[9] G. Park, H. Cudney, D. J. Inman, ASCE J. Infrast. Syst., Vol. 6, No. 4, (2000), 153.
[10] C. K. Soh, K. Tseng, S. Bhalla and A. Gupta, Smart Mater. Struct., V9, 2000, 533.
[11] G. Park, H. Cudney, D. J. Inman, Earthquake Eng. Struct. Dyn. J., Vol. 30, No. 10, 2001, 1463.
[12] Corey Wilson Pitchford, "Impedance-based structural health monitoring Wind Turbine Blades", Mater's Thesis, Center Intell. Mater. Syst. Struct., Virginia Polytech. Inst. State University, (2008).
[13] K. J. Xing and C. P. Fritzen, Key Eng. Mater., vol. 347, 2007, 153.
[14] Y. Yang and Y. Hu, Smart Mater. Struct., vol. 17, no. 1, Article ID 015005, 11 pages, 2008.
[15] Park, Seunghee, and Sun-Kyu Park., Res. Nondestr. Eval., 21.3 (2010): 184.
[16] Sepehry, Naserodin, M. Shamshirsaz, and A. Bastani., Struct. Health Monit., 10.6 (2011): 573.
[17] Grard, Charles Albert Marie. Aluminum and its alloys. 1922.
[18] B. Akhoundi, M. A. Shamshirsaz, S. R. Hamzehlou and F. Hajami, "Real-time health monitoring and fault detection due to the corrosion of aluminum tubes by electrical impedance", 6th condition monitoring and fault diagnosis conference (CMFD2012), 2012. (in Persian)
[19] F. G. Baptista, D. Budoya, Vinicius A D de Almeidal and Jose Alfredo C Ulson, Sens., 14.1 (2014): 1208.
[20] C. Rugina, A. Toader, V. Giurgiutiu and I. Ursu, Proc. Romanian Acad., Ser. A, Math., Phys., Tech. Sci., Inf. Sci., 15.3 (2014): 272.
[21] F. Sun, Z. Chaudhry, C. Liang and Rogers, J. Intell. Mater. Syst. Struct., Vol. 6, 134.
[22] S. O. R. Moheimani and A. J. Fleming, Adv. Ind. Control, London: Springer-Verlag, (2006).